



Available online at www.sciencedirect.com

SCIENCE @ DIRECT®

C. R. Chimie 8 (2005) 1543–1551



<http://france.elsevier.com/direct/CRAS2C/>

Full paper / Mémoire

Self-assembly of hybrid solids consisting of 2D supramolecular networks and intercalated metal complexes

Myunghyun Paik Suh *, Joong Won Jeon, Hoi Ri Moon, Kil Sik Min, Hye Jin Choi

Department of Chemistry, Seoul National University, Seoul 151-747, South Korea

Received 31 March 2004; accepted 11 October 2004

Available online 22 April 2005

Abstract

Hybrid compounds $[\text{NaCr}(\text{ox})_3]_2[\text{Ni}(\text{cyclam})][\text{Ni}(\text{cyclam})(\text{H}_2\text{O})_2] \cdot 8 \text{H}_2\text{O}$ (**1**) and $[\text{NaCr}(\text{ox})_3][\text{Cu}(\text{tren})(\text{H}_2\text{O})] \cdot 3 \text{H}_2\text{O}$ (**2**) are assembled in MeCN/H₂O from the reaction of $\text{Na}_3[\text{Cr}(\text{ox})_3] \cdot 5 \text{H}_2\text{O}$ with $[\text{Ni}(\text{cyclam})](\text{ClO}_4)_2$ and $[\text{Cu}(\text{tren})](\text{PF}_6)_2$, respectively, where cyclam = 1,4,8,11-tetraazacyclotetradecane and tren = tris(2-aminoethyl)amine. In **1** and **2**, Ni(II) macrocyclic complex and Cu(II) complex, respectively, are intercalated between the anionic 2D layers of $[\text{NaCr}(\text{ox})_3]_n^{2n-}$. The magnetic susceptibility data of **1** and **2**, measured in the temperature range 5–301 K, indicate weak ferromagnetic interactions ($\theta = 1.9 \text{ K}$ for **1** and 0.29 K for **2**) between the Cr(III) ions in the 2D layers and the intercalated paramagnetic metal complexes. **To cite this article:** *M.P. Suh et al., C. R. Chimie 8 (2005).*

© 2005 Académie des sciences. Published by Elsevier SAS. All rights reserved.

Résumé

Des composés hybrides $[\text{NaCr}(\text{ox})_3]_2[\text{Ni}(\text{cyclam})][\text{Ni}(\text{cyclam})(\text{H}_2\text{O})_2] \cdot 8 \text{H}_2\text{O}$ (**1**) et $[\text{NaCr}(\text{ox})_3][\text{Cu}(\text{tren})(\text{H}_2\text{O})] \cdot 3 \text{H}_2\text{O}$ (**2**) sont assemblés dans une mixture de MeCN/H₂O à partir de la réaction de $\text{Na}_3[\text{Cr}(\text{ox})_3] \cdot 5 \text{H}_2\text{O}$ avec $[\text{Ni}(\text{cyclam})](\text{ClO}_4)_2$ et $[\text{Cu}(\text{tren})](\text{PF}_6)_2$, où cyclam = 1,4,8,11-tétraazacyclotétradécane et tren = tris(2-aminoéthyl)amine. Dans **1** et **2**, le complexe macrocyclic Ni(II) et le complexe Cu(II) sont respectivement intercalés entre les couches anioniques 2D de $[\text{NaCr}(\text{ox})_3]_n^{2n-}$. La susceptibilité magnétique des données de **1** et **2**, mesurée dans une fourchette de 5–301 K, indique des interactions ferromagnétiques faibles ($\theta = 1.9 \text{ K}$ pour **1** et 0.29 K pour **2**) entre les ions Cr(III) dans les couches 2D et les complexes métalliques paramagnétiques intercalés. **Pour citer cet article :** *M.P. Suh et al., C. R. Chimie 8 (2005).*

© 2005 Académie des sciences. Published by Elsevier SAS. All rights reserved.

Keywords: Chromium oxalate; Copper complex; 2D network; Hybrid compounds; Intercalation; Nickel macrocycle; Self-assembly

Mots clés : Oxalate de chrome ; Complexes de cuivre ; Réseau 2D ; Composés hybrides ; Intercalation ; Macrocycle de nickel ; Auto-assemblage

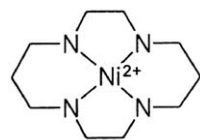
* Corresponding author.

E-mail address: mpsuh@snu.ac.kr (M.P. Suh).

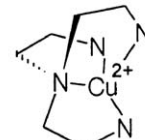
1. Introduction

Crystal engineering has provided chemists with a useful paradigm for the rational design of solid-state structures [1]. In particular, self-assembly of pre-selected molecular building blocks may yield designed supramolecular structure in one-pot process. We have been interested in construction of the materials, where two species with different properties coexist in the same crystal lattice [2,3], based on crystal engineering and host–guest interactions. In particular, intercalation of transition metal complexes between the supramolecular layers is interesting because it might implicate efficient methods for removing heavy metal ions from the pollutant and/or developing the solid catalysts. Although transition metal complexes have often been inserted into the inorganic layered hosts such as double hydroxides [4,5], they are inserted into 2D metal–organic supramolecular networks in the limited cases: $[M^{III}(Cp_2^*)]^+$ ($M = Co, Fe$; $Cp^* =$ pentamethylcyclopentadienyl) [6,7] and $[M(bpy)_3]^{2+}$ ($bpy = 2,2'$ -bipyridine) [8–12] have been inserted between the coordination polymer layers of $[M^II Cr^{III}(ox)_3]_n^{n-}$ [6–9] ($M^II = Mn, Fe, Co, Ni, Cu$ and Zn ; $ox =$ oxalate) or $[M^I M^{III}(ox)_3]_n^{2n-}$ [10–12] ($M^I = Li, Na, K$; $M^{III} = Cr, Fe$). In particular, tris(oxalate)metallate networks formed by $[A^I M^{II}(ox)_3]^{2-}$ ($A^I = H_3O^+, NH_4^+$; $M^{II} = Cr, Fe, Ga$) have been employed to prepare molecular conducting materials [13,14] and those by monoanionic $[M^II M^{III}(ox)_3]^-$ networks ($M^II = Cr, Mn, Fe, Co, Ni, Cu$; $M^{III} = Cr, Fe$) have been used to intercalate organic cation or decamethylferrocenium ion [15–20]. The oxalate based materials showed interesting optical and magnetic properties [21–23].

Here we report self-assembly of compounds, $[NaCr(ox)_3]_2[Ni(cyclam)][Ni(cyclam)(H_2O)_2] \cdot 8 H_2O$ (**1**) and $[NaCr(ox)_3][Cu(tren)(H_2O)] \cdot 3 H_2O$ (**2**), in which transition metal complexes, $[Ni(cyclam)]^{2+}$ and $[Cu(tren)]^{2+}$ ($cyclam = 1,4,8,11$ -tetraazacyclotetradecane and $tren =$ tris(2-aminoethyl)amine), respectively, are intercalated between the 2D metal–organic layers of $[NaCr(ox)_3]_n^{2n-}$. We chose $[Ni(cyclam)](ClO_4)_2$ and $[Cu(tren)](PF_6)_2$ as the intercalating complexes because the former was involved in the olefin epoxidation [24] and CO_2 reduction [25] as a catalyst, and the latter in ligand-substitution reaction [26]. The solid intercalating these complexes might have potentials to be used as solid catalyst.



$[Ni(cyclam)]^{2+}$



$[Cu(tren)]^{2+}$

2. Experimental

2.1. Materials

All chemicals and solvents used in the synthesis were of the reagent grade and used without further purification. $Na_3[Cr(ox)_3] \cdot 5 H_2O$ [27], $[Ni(cyclam)](ClO_4)_2$ [28], and $[Cu(tren)](PF_6)_2 \cdot H_2O$ [29] were prepared according to the literature.

2.2. Measurement

Infrared spectra were recorded with a Perkin Elmer 2000 FT-IR spectrophotometer. UV/vis diffuse reflectance spectra were recorded with a Cary 300 Bio UV/vis spectrometer. Elemental analysis was performed by the analytical laboratory of Seoul National University. Thermogravimetric analysis (TGA) was performed under $N_2(g)$ at a scan rate of $5^\circ C min^{-1}$ using a Dupont TGA 2050 instrument. Magnetic susceptibility was measured on a Quantum Design MPMS superconducting quantum interference device (SQUID) at Korea Basic Science Institute, Daejeon.

2.3. Synthesis

2.3.1. $[NaCr(ox)_3]_2[Ni(cyclam)][Ni(cyclam)(H_2O)_2] \cdot 8 H_2O$ (**1**)

An MeCN/ H_2O (1:2 v/v, 10 ml) solution of $[Ni(cyclam)](ClO_4)_2$ (0.92 g, 2 mmol) was added dropwise to the aqueous solution (5 ml) of $Na_3[Cr(ox)_3] \cdot 5 H_2O$ (0.73 g, 2 mmol) at room temperature. The solution was allowed to stand at room temperature until greenish brown crystals formed, which were filtered off, washed with EtOH, and dried in air. Yield: 87%. Elemental analysis calcd for $C_{32}H_{68}Cr_2N_8Na_2Ni_2O_{34}$: C 27.93, H 4.98, N 8.14; found: C 28.39, H 4.70, N 8.48. FT-IR (Nujol mull): 3396(s), 3151(s), 1704(s), 1651(s), 1263(s), 1101(s), 1072(s), 1053(s), 898(s), 819(s), 803(s), 543(s) cm^{-1} . UV/vis (diffuse reflectance spectrum): $\lambda_{max} = 424, 565$ nm.

2.3.2. $[\text{NaCr}(\text{ox})_3][\text{Cu}(\text{tren})(\text{H}_2\text{O})]\cdot 3\text{H}_2\text{O}$ (**2**)

An MeCN/H₂O (10 ml, 1:1 v/v) solution of $[\text{Cu}(\text{tren})](\text{PF}_6)_2\cdot\text{H}_2\text{O}$ (1.00 g, 2 mmol) was added dropwise to the aqueous solution (5 ml) of $\text{Na}_3[\text{Cr}(\text{ox})_3]\cdot 5\text{H}_2\text{O}$ (0.73 g, 2 mmol) at room temperature. The solution was allowed to stand at room temperature until bluish green crystals formed, which were filtered off, washed with diethyl ether, and dried in air. Yield: 90%. Elemental analysis calcd for $\text{C}_{12}\text{H}_{26}\text{CrCuN}_4\text{NaO}_{16}$: C 23.21, H 4.22, N 9.02; found: C 23.28, H 4.17, N 9.15. FT-IR (Nujol mull): 3466(br, s), 3353(s), 3296(s), 3169(s), 1705(s), 1651(s), 1596(s), 1263(s), 898(s), 816(s), 802(s), 541(s) cm^{-1} . UV/vis (diffuse reflectance spectrum, λ_{max}): 420, 593 nm.

2.4. X-ray diffraction measurement

Single crystals of **1** and **2** were sealed in glass capillary tubes with their mother liquor, and X-ray diffraction data were collected at 100 K with an Enraf–Nonius Kappa CCD diffractometer (Mo $K\alpha$, $\lambda = 0.71073$ Å, graphite monochromator). Preliminary orientation matrices and unit cell parameters were obtained from the peaks of the first 10 frames and were then refined using the whole data set. Frames were integrated and corrected for Lorenz and polarization effects using DENZO [30]. The scaling and the global refinement of crystal parameters were performed by SCALEPACK. No absorption correction was made. The crystal structures were solved by the direct methods [31] and refined by full-matrix least-squares refinement using the SHELXL97 computer program [32]. The positions of all non-hydrogen atoms were refined with anisotropic displacement factors. The hydrogen atoms were positioned geometrically and refined using a riding model. The crystallographic data for **1** and **2** are summarized in Table 1 and the selected bond lengths and angles are shown in Tables 2 and 3.

3. Results and discussion

3.1. Self-assembly and properties of **1** and **2**

$[\text{NaCr}(\text{ox})_3]_2[\text{Ni}(\text{cyclam})][\text{Ni}(\text{cyclam})(\text{H}_2\text{O})_2]\cdot 8\text{H}_2\text{O}$ (**1**) and $[\text{NaCr}(\text{ox})_3][\text{Cu}(\text{tren})(\text{H}_2\text{O})]\cdot 3\text{H}_2\text{O}$ (**2**) were prepared by mixing the aqueous solution of

$\text{Na}_3[\text{Cr}(\text{ox})_3]\cdot 5\text{H}_2\text{O}$ with the MeCN/H₂O (1:1 v/v) solutions of $[\text{Ni}(\text{cyclam})](\text{ClO}_4)_2$ and $[\text{Cu}(\text{tren})](\text{PF}_6)_2\cdot\text{H}_2\text{O}$, respectively, at room temperature. The solids **1** and **2** are insoluble in any solvents except in water as evidenced by UV/vis spectra measured for the solvents in which the solids were immersed for 24 h. Thermal gravimetric analysis (TGA) of **1** indicates that all water guest molecules (10.5%) are removed continuously at 23–89 °C, and the remaining compound can be heated up to 300 °C without any additional weight loss. The IR spectrum of solid **1** dried at 250 °C for 1.5 h still showed water peaks, indicating that the coordinated water molecules are intact at this temperature. TGA trace of **2** shows that all guest water molecules (8.6%) are removed at 23–105 °C and the coordinated water molecule (3%) at 105–153 °C, and the rest of the compound is stable up to 230 °C (Fig. 1).

3.2. X-ray crystal structure of **1**

In the structure of **1** (Fig. 2), dipositive metal complexes are intercalated between the negatively charged 2D layers (designated as A) of $[\text{NaCr}(\text{ox})_3]_n^{2n-}$. Within a $[\text{NaCr}(\text{ox})_3]_n^{2n-}$ layer, $\text{Cr}(\text{ox})_3^{3-}$ units are linked by Na(I) ions to form a circular supramolecular synthon made of three Cr(III) ions and three Na(I) ions. Each Cr(III) ion is coordinated by six oxygen atoms of three oxalate anions to display trigonally distorted octahedral coordination geometry (av. Cr–O_{ox} bond distance, 1.975(1) Å). Each Na(I) ion is surrounded by six oxygen atoms of three $[\text{Cr}(\text{ox})_3]^{3-}$ units, which are not coordinating Cr(III) ion. Therefore, each oxalate ligand is linked to one Cr(III) and one Na(I) ion. The average

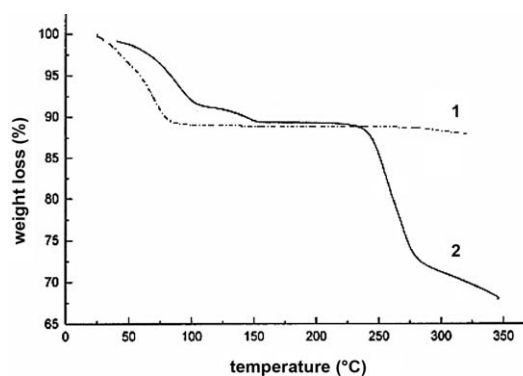


Fig. 1. TGA traces for $[\text{NaCr}(\text{ox})_3]_2[\text{Ni}(\text{cyclam})][\text{Ni}(\text{cyclam})(\text{H}_2\text{O})_2]\cdot 8\text{H}_2\text{O}$ (**1**) and $[\text{NaCr}(\text{ox})_3][\text{Cu}(\text{tren})(\text{H}_2\text{O})]\cdot 3\text{H}_2\text{O}$ (**2**).

Table 1

Crystallographic data for [NaCr(ox)₃]₂[Ni(cyclam)][Ni(cyclam)(H₂O)₂]₈·8 H₂O (**1**) and [NaCr(ox)₃][Cu(tren)(H₂O)]₃·3 H₂O (**2**)

Empirical formula	C ₃₂ H ₆₈ Cr ₂ N ₈ Na ₂ Ni ₂ O ₃ (1)	C ₁₂ H ₂₆ Cr ₁ Cu ₁ N ₄ Na ₁ O ₁₆ (2)
<i>F</i> _w	1376.34	620.90
Crystal size (mm ³)	0.3 × 0.3 × 0.2	0.2 × 0.2 × 0.3
Crystal system	Triclinic	Monoclinic
Space group	<i>P</i> $\bar{1}$	<i>P</i> 2 ₁ / <i>c</i>
Unit cell dimensions		
<i>a</i> (Å)	9.565(0)	9.389
<i>b</i> (Å)	9.829(0)	17.477(1)
<i>c</i> (Å)	18.272(1)	16.376(1)
α (°)	91.057(1)	90.000
β (°)	104.607(2)	103.185(1)
γ (°)	118.210(2)	90.000
<i>V</i> (Å ³)	1445.65(8)	2616.3(2)
<i>Z</i>	1	4
<i>D</i> _{calc} (g cm ⁻³)	1.581	1.576
Absorption coefficient (mm ⁻¹)	1.121	1.319
<i>F</i> (000)	714	1272
Measurement temperature (K)	100(2)	100(2)
λ (Å)	0.71073	0.71073
θ Range for data collection (°)	3.06–27.60	3.28–26.95
Index ranges	–11 ≤ <i>h</i> ≤ 12 –12 ≤ <i>k</i> ≤ 12 –23 ≤ <i>l</i> ≤ 23	–11 ≤ <i>h</i> ≤ 12 –21 ≤ <i>k</i> ≤ 19 –19 ≤ <i>l</i> ≤ 19
Reflections collected	9146	8696
Independent reflections	6576 [<i>R</i> _{int} = 0.0303]	4718 [<i>R</i> _{int} = 0.0639]
Refinement method	Full-matrix least-squares on <i>F</i> ²	Full-matrix least-squares on <i>F</i> ²
Data/restraints/parameters	6576/0/364	4718/0/316
Goodness-of-fit	1.059	1.013
Final <i>R</i> indices [<i>I</i> > 2 σ (<i>I</i>)] ^a	<i>R</i> ₁ = 0.0565, <i>wR</i> ₂ = 0.1667	<i>R</i> ₁ = 0.0725, <i>wR</i> ₂ = 0.2042
<i>R</i> indices (all data)	<i>R</i> ₁ = 0.0898, <i>wR</i> ₂ = 0.1765	<i>R</i> ₁ = 0.1606, <i>wR</i> ₂ = 0.2263
Largest difference in peak and hole (e Å ⁻³)	0.847 and –0.810	0.714 and –0.648

^a $R_1 = \sum \|F_o\| - |F_c| / \sum |F_o| wR_2(F^2) = [\sum w(|F_o|^2 - |F_c|^2)^2 / \sum w(|F_o|^4)]^{1/2}$, where:
 $w = 1/[\sigma^2(F_o^2) + (0.0984 P)^2 + 0.33 P]$, where $P = (\max(F_o^2, 0) + 2 F_c^2)/3$ for **1**;
 $w = 1/[\sigma^2(F_o^2) + (0.1179 P)^2 + 0.00 P]$, where $P = (\max(F_o^2, 0) + 2 F_c^2)/3$ for **2**.

Na...O_{ox} distance is 2.383(1) Å, which is close to the sum (2.42 Å) of ionic radii but significantly shorter than the sum of their van der Waals radii (2.80 Å) [33]. The 2D layers (A) extend parallel to the *ab* plane and they are stacked alternately in a slipped manner (AA'AA'AA'...). Between the [NaCr(ox)₃]_n²ⁿ⁻ layers, the diamagnetic four-coordinate [Ni(cyclam)]²⁺ complexes (designated as B) and the paramagnetic six-coordinate [Ni(cyclam)(H₂O)₂]²⁺ complexes (designated as C) are alternately intercalated in the ...ABA'CABA'C... sequence. The shortest Cr...Cr distance within a layer is 9.565(0) Å. The distances between the two 2D layers intercalating [Ni(cyclam)]²⁺ and [Ni(cyclam)(H₂O)₂]²⁺ units are 8.582(1) and

8.867(1) Å, respectively. The shortest distances between Cr atom of the 2D network and the Ni atom in B and C cationic complex layers are 5.485(1) and 6.415(1) Å, respectively. The macrocyclic coordination planes of [Ni(cyclam)]²⁺ and [Ni(cyclam)(H₂O)₂]²⁺ are tilted with respect to the anionic [NaCr(ox)₃]_n²ⁿ⁻ layers with the dihedral angles of 35.0° and 77.1°, respectively. The 2D coordination polymer layers and the intercalated macrocyclic complexes are linked by the hydrogen bonding interactions, involving the oxygen atom of oxalate anion and the secondary amine of macrocycle (N4...O1(*x*, *y* – 1, *z*), 2.981(5) Å; \angle N4–H4–O1(*x*, *y* – 1, *z*), 162.5°). Eight water molecules per unit formula of **1** are included between the 2D layers along with the

Table 2

Selected bond distances (Å) and angles (°) for [NaCr(ox)₃]₂[Ni(cyclam)][Ni(cyclam)(H₂O)₂]-8 H₂O (**1**)

<i>Bond distances</i>			
Cr(1)–O(1)	1.980(3)	Na(1)–O(3)	2.351(3)
Cr(1)–O(2)	1.972(3)	Na(1)–O(4)	2.430(3)
Cr(1)–O(5)	1.973(3)	Na(1)–O(7) ^a	2.392(3)
Cr(1)–O(6)	1.983(3)	Na(1)–O(8) ^a	2.361(3)
Cr(1)–O(9)	1.968(3)	Na(1)–O(11) ^b	2.382(3)
Cr(1)–O(10)	1.972(3)	Na(1)–O(12) ^b	2.379(3)
Ni(1)–N(2)	2.065(3)	Ni(2)–N(3)	1.932(4)
Ni(1)–N(1)	2.071(3)	Ni(2)–N(4)	1.934(4)
Ni(1)–O(1W)	2.169(3)		
<i>Bond angles</i>			
O(1)–Cr(1)–O(2)	82.72(11)	O(6)–Cr(1)–O(9)	173.9(12)
O(1)–Cr(1)–O(5)	89.66(12)	O(6)–Cr(1)–O(10)	92.74(11)
O(1)–Cr(1)–O(6)	92.09(11)	O(9)–Cr(1)–O(10)	82.53(11)
O(1)–Cr(1)–O(9)	92.85(11)	N(2)–Ni(1)–N(2) ^c	180.0(2)
O(1)–Cr(1)–O(10)	174.34(11)	N(1)–Ni(1)–N(1) ^c	180.00(19)
O(2)–Cr(1)–O(5)	171.44(12)	N(2)–Ni(1)–N(1)	85.45(14)
O(2)–Cr(1)–O(6)	93.48(11)	N(2) ^c –Ni(1)–N(1)	94.55(14)
O(2)–Cr(1)–O(9)	90.70(12)	O(3)–Na(1)–O(4)	71.03(11)
O(2)–Cr(1)–O(10)	94.04(14)	O(3)–Na(1)–O(7) ^a	71.25(12)
O(5)–Cr(1)–O(6)	82.86(11)	O(3)–Na(1)–O(8) ^a	89.81(13)
O(5)–Cr(1)–O(9)	93.58(12)	O(3)–Na(1)–O(11) ^b	103.08(12)
O(5)–Cr(1)–O(10)	93.87(12)	O(3)–Na(1)–O(12) ^b	170.04(12)
O(7) ^a –Na(1)–O(4)	157.75(13)	O(12) ^b –Na(1)–O(4) ^a	101.07(12)
O(8) ^a –Na(1)–O(4)	94.99(12)	O(12) ^b –Na(1)–O(7) ^a	97.79(12)
O(8) ^a –Na(1)–O(7) ^a	70.93(10)	O(12) ^b –Na(1)–O(11) ^b	71.42(11)
O(8) ^a –Na(1)–O(11) ^b	164.27(13)	N(1)–Ni(1)–OW1	90.28(13)
O(8) ^a –Na(1)–O(12) ^b	97.05(12)	N(3) ^d –Ni(2)–N(3)	180.00(15)
O(11) ^b –Na(1)–O(4) ^a	97.70(13)	N(3) ^d –Ni(2)–N(4)	93.29(16)
O(11) ^b –Na(1)–O(7) ^a	99.43(12)	N(3)–Ni(2)–N(4)	86.71(16)

Symmetry transformations used to generate equivalent atoms.

^a $x - 1, y, z$.^b $x, y + 1, z$.^c $-x + 1, -y, -z$.^d $-x + 1, -y, -z + 1$.

metal complexes. The coordinated water (OW1) of Ni(II)-cyclam complex and the guest water molecules form hydrogen bonds with the oxygen atoms of oxalate anions, the secondary amines of the macrocycles, and the other water guest molecules.

3.3. X-ray crystal structure of **2**

In the structure of **2** (Fig. 3), positively charged [Cu(tren)(H₂O)]²⁺ complexes are intercalated between the 2D layers of [NaCr(ox)₃]_n²ⁿ⁻, similarly to **1**. The average Cr–O_{ox} bond and Na⋯O_{ox} distances are 1.971(2) and 2.386(2) Å, respectively. The 2D layers

extend parallel to the *ab* plane. The shortest Cr⋯Cr distance within the [NaCr(ox)₃]_n²ⁿ⁻ layer is 9.389(0) Å. The [NaCr(ox)₃]_n²ⁿ⁻ layers (A) are stacked in a slipped manner and the [Cu(tren)(H₂O)]²⁺ complexes (B) are intercalated between the layers of A in the ⋯ABA-BAB⋯ sequence. The interlayer distance is 8.049(1) Å. The Cu(II) ion of [Cu(tren)(H₂O)]²⁺ has a distorted trigonal bipyramidal coordination geometry. The dihedral angle between the trigonal plane of Cu(II) complex and the 2D layer is 55.8°. Within a layer B, the shortest Cu⋯Cu distance is 8.189(2) Å. The shortest Cr⋯Cu distance between the two different layers is 5.406(2) Å. The 2D [NaCr(ox)₃]_n²ⁿ⁻ layers and the

Table 3

Selected bond distances (Å) and angles (°) for [NaCr(ox)₃][Cu(C₆H₁₈N₄)(H₂O)]·3 H₂O (**2**)

<i>Bond distances</i>			
Cr(1)–O(1)	1.965(5)	Na(1)–O(3) ^a	2.388(6)
Cr(1)–O(2)	1.995(5)	Na(1)–O(4) ¹	2.333(5)
Cr(1)–O(5)	1.985(5)	Na(1)–O(7)	2.369(6)
Cr(1)–O(6)	1.967(4)	Na(1)–O(8)	2.428(5)
Cr(1)–O(9)	1.959(5)	Na(1)–O(11) ^b	2.437(6)
Cr(1)–O(10)	1.957(5)	Na(1)–O(12) ^b	2.371(6)
Cu(1)–N(1)	2.034(6)	Cu(1)–N(3)	1.985(6)
Cu(1)–N(2)	2.159(6)	Cu(1)–N(4)	2.019(6)
Cu(1)–OW1	2.009(6)		
<i>Bond angles</i>			
O(1)–Cr(1)–O(2)	82.84(19)	O(10)–Cr(1)–O(5)	174.4(2)
O(1)–Cr(1)–O(5)	91.4(2)	O(10)–Cr(1)–O(6)	94.0(2)
O(1)–Cr(1)–O(6)	171.0(2)	O(10)–Cr(1)–O(9)	83.6(2)
O(5)–Cr(1)–O(2)	92.5(2)	N(1)–Cu(1)–N(2)	105.4(3)
O(6)–Cr(1)–O(2)	90.7(2)	N(3)–Cu(1)–N(1)	85.4(2)
O(6)–Cr(1)–O(5)	82.6(2)	N(3)–Cu(1)–N(2)	85.6(3)
O(9)–Cr(1)–O(1)	94.1(2)	N(3)–Cu(1)–N(4)	85.2(3)
O(9)–Cr(1)–O(2)	174.5(2)	N(4)–Cu(1)–N(2)	109.7(3)
O(9)–Cr(1)–O(5)	92.1(2)	O(3) ^a –Na(1)–O(4) ^a	72.26(19)
O(9)–Cr(1)–O(6)	92.8(2)	O(3) ^a –Na(1)–O(8)	91.6(2)
O(10)–Cr(1)–O(1)	92.6(2)	O(3) ^a –Na(1)–O(11) ^b	163.0(2)
O(10)–Cr(1)–O(2)	92.0(2)	O(4) ^a –Na(1)–O(7)	155.4(2)
O(4) ^a –Na(1)–O(8)	89.2(2)	O(12) ^b –Na(1)–O(3) ^a	94.6(2)
O(4) ^a –Na(1)–O(11) ^b	101.3(2)	O(12) ^b –Na(1)–O(8)	171.7(2)
O(4) ^a –Na(1)–O(12) ^b	98.0(2)	O(12) ^b –Na(1)–O(11) ^b	70.4(2)
O(7)–Na(1)–O(3) ^a	95.1(2)	N(4)–Cu(1)–N(1)	142.8(3)
O(7)–Na(1)–O(8)	69.75(18)	OW1–Cu(1)–N(3)	173.6(3)
O(7)–Na(1)–O(11) ^b	96.2(2)	OW1–Cu(1)–N(4)	92.5(3)
O(7)–Na(1)–O(12) ^b	104.2(2)	OW1–Cu(1)–N(1)	92.9(3)
O(8)–Na(1)–O(11) ^b	104.2(2)	OW1–Cu(1)–N(2)	100.7(3)

Symmetry transformations used to generate equivalent atoms.

^a $x - 1, y, z.$ ^b $-x + 1, y + 1/2, -z.$

intercalated Cu(II) complexes are linked by the hydrogen bonding interactions, involving oxalate oxygen atoms that are linked to Na(I) ion and the primary amine groups of the [Cu(tren)]²⁺ unit {N1...O11($x, -y + 1/2, z + 1/2$), 3.060(8) Å; ∠N1–H1A–O11, 149.9°; N1...O8, 3.074(8) Å; ∠N1–H1B–O8, 163.3°; N2...O3($x - 1, -y + 1/2, z + 1/2$), 3.083(9) Å; ∠N2–H2A–O3, 156.5°}. Three water molecules per unit formula are included between the 2D layers.

3.4. Magnetic properties of **1** and **2**

The magnetic susceptibility data of **1** and **2** were measured in the temperature range 5–301 K at an

applied field of 5000 G (Fig. 4). $\chi_M T$ vs. T plot for **1** shows weak ferromagnetism at 16–301 K, but $\chi_M T$ value slightly decreases below 16 K. The plot of $1/\chi_M$ vs. T is linear to provide excellent fit to the Curie–Weiss law, $1/\chi_M = (T - \theta)/C$. Curie constant C and Weiss temperature θ are estimated from the data, which yields C value of 4.72 cm³ K mol⁻¹ and θ value of 1.9 K for **1**. Compound **2** also shows a weak ferromagnetism at 7–301 K, which provides C of 2.44 cm³ K mol⁻¹ and θ of 0.29 K. The θ value decreases when going from **1** to **2** because spin number of Cu(II) in **2** is smaller than Ni(II) in **1**. The weak ferromagnetic interactions in these compounds must be attributed to the long Cr(III)···Cr(III) distances within the [NaCr(ox)₃]_n²ⁿ⁻

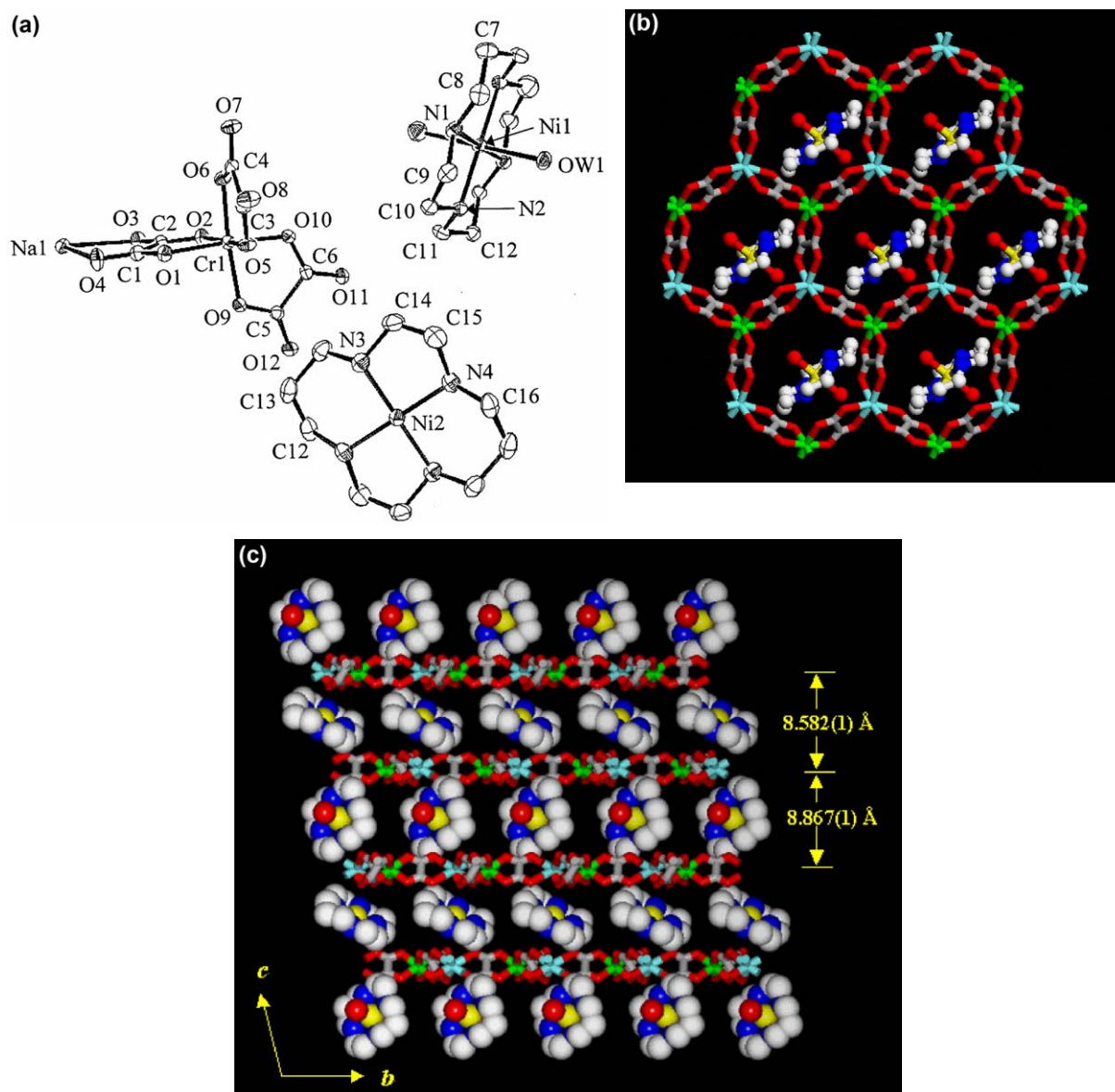


Fig. 2. X-ray crystal structure of $[\text{NaCr}(\text{ox})_3]_2[\text{Ni}(\text{cyclam})][\text{Ni}(\text{cyclam})(\text{H}_2\text{O})_2] \cdot 8 \text{H}_2\text{O}$ (**1**), showing (a) an ORTEP drawing, (b) top view of the packed structure, (c) side view of the packed structure. Yellow, nickel ion; blue, nitrogen; gray, carbon; red, oxygen; white, sodium ion; green, chromium ion; pink, oxygen of oxalate. Guest molecules and hydrogen atoms are omitted for clarity.

layer and the long $\text{Ni}(\text{II}) \cdots \text{Ni}(\text{II})$ and $\text{Cu}(\text{II}) \cdots \text{Cu}(\text{II})$ distances between the intercalated complexes as well as the long distances between $\text{Cr}(\text{III})$ and intercalated metal ions, $\text{Ni}(\text{II})$ and $\text{Cu}(\text{II})$.

4. Conclusion

We have assembled and characterized new solids consisting of negatively charged $[\text{NaCr}(\text{ox})_3]_n^{2n-}$ lay-

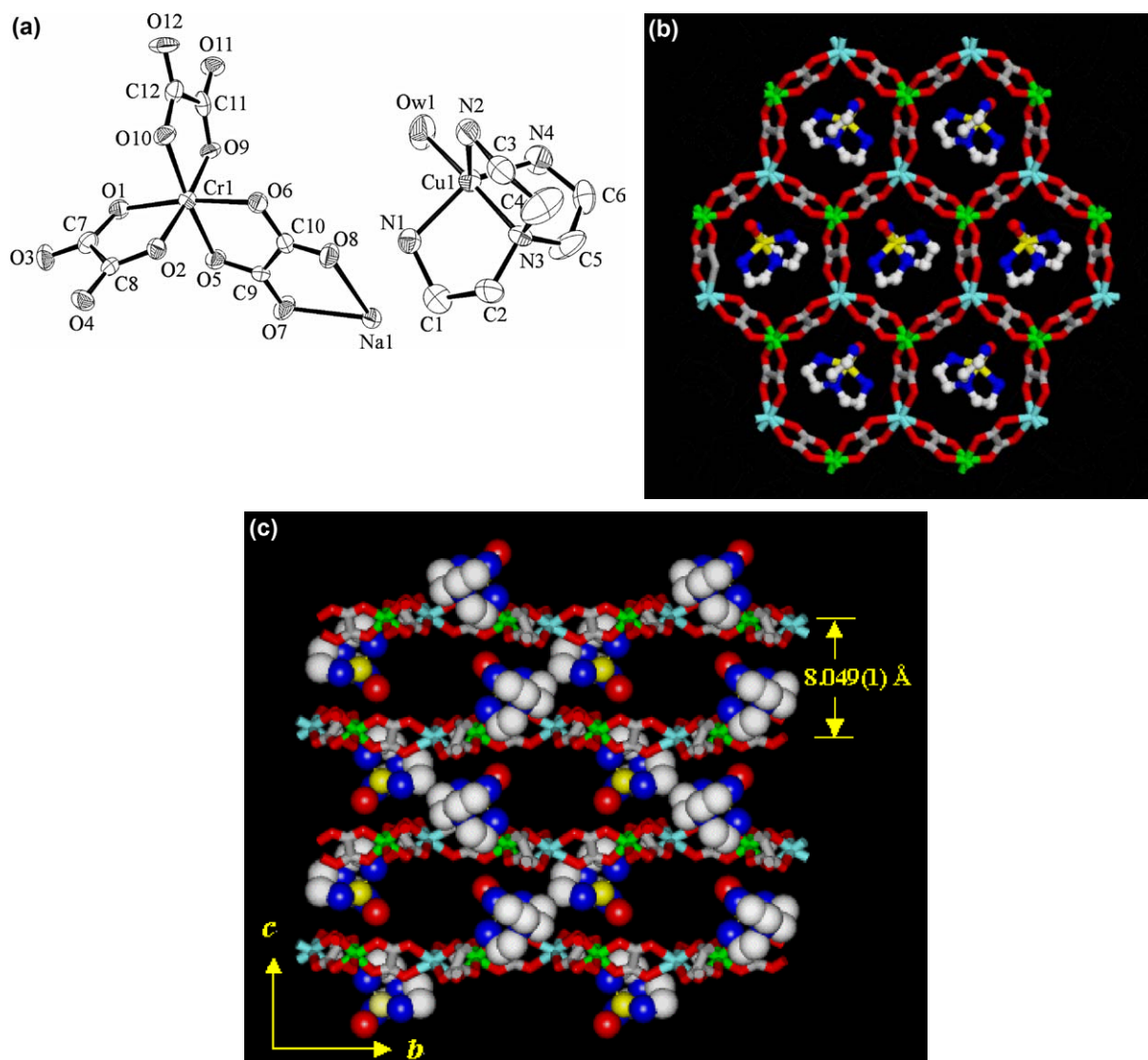


Fig. 3. X-ray crystal structure of $[\text{NaCr}(\text{ox})_3][\text{Cu}(\text{tren})(\text{H}_2\text{O})] \cdot 3 \text{H}_2\text{O}$ (**2**), showing (a) an ORTEP drawing, (b) top view of the packed structure, (c) side view of the packed structure. Yellow, copper; blue, nitrogen; gray, carbon; red, oxygen; white, sodium; green, chromium; pink, oxygen of oxalate. Guest molecules and hydrogen atoms are omitted for clarity.

ers and the intercalated complexes, $[\text{Ni}(\text{cyclam})]^{2+}$ and $[\text{Cu}(\text{tren})]^{2+}$. This work illustrates new types of solid, whose property may be applied to selective removal of heavy metal ions. The versatility in the aza-macrocyclic ligand, in terms of the possibility of functionalizing the ring, also can be utilized to prepare solids of different compositions and structural architectures. We are cur-

rently carrying out the experiments testing if **1** and **2** can be applied to solid catalysts.

5. Supplementary material

Crystallographic data for the structural analysis of **1** and **2** have been deposited with the Cambridge Crys-

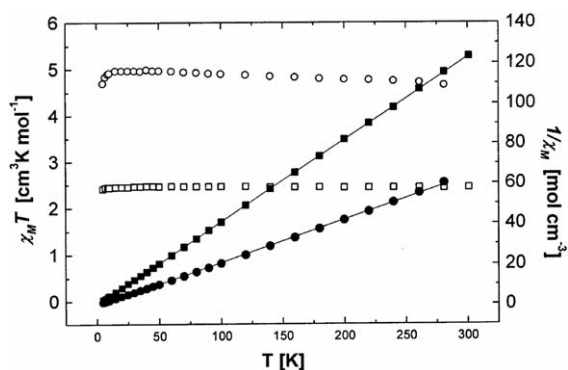


Fig. 4. Temperature dependent $\chi_M T$ and the inverse susceptibility $1/\chi_M$ per formula unit of $[\text{NaCr}(\text{ox})_3]_2[\text{Ni}(\text{cyclam})][\text{Ni}(\text{cyclam})\cdot(\text{H}_2\text{O})_2]\cdot 8 \text{H}_2\text{O}$ (**1**) (\circ , \bullet) $[\text{NaCr}(\text{ox})_3][\text{Cu}(\text{tren})(\text{H}_2\text{O})]\cdot 3 \text{H}_2\text{O}$ (**2**) (\square , \blacksquare).

talographic Data Center, CCDC No. 202101 for compound **1** and CCDC No. 202102 for **2**. Copies of this information may be obtained free of charge from The Director, CCDC, 12 Union Road, Cambridge CB21EZ, UK (fax: +44 1223 336 033; e-mail: deposit@ccdc.cam.ac.uk or www.ccdc.cam.ac.uk).

Acknowledgements

This work was supported by Korea Institute of S&T Evaluation and Planning (Project No. M1-0213-03-0001).

References

- [1] G.R. Desiraju, *Nature* 412 (2001) 397.
- [2] E. Coronado, J.R. Galán-Mascarós, C.J. Gómez-García, V. Laukhin, *Nature* 408 (2000) 447.
- [3] J.W. Ko, K.S. Min, M.P. Suh, *Inorg. Chem.* 41 (2002) 2151.
- [4] V. Prevot, D. Forando, J.-P. Besse, *J. Solid-State Chem.* 153 (2000) 301.
- [5] C.A.S. Barbosa, A.M.D.C. Ferreira, V.R.L. Constantino, *J. Incl. Phenom. Macro.* 42 (2002) 15.
- [6] E. Coronado, J.-R. Galan-Mascaros, C.-J. Gomez-Garcia, J. Ensling, P. Gutlich, *Chem. Eur. J.* 6 (2000) 552.
- [7] E. Coronado, J.R. Galan-Mascaros, C.J. Gomez-Garcia, J.M. Martinez-Agudo, E. Martinez-Ferrero, J.C. Waerenborgh, M. Almeida, *J. Solid-State Chem.* 159 (2001) 391.
- [8] E. Coronado, J.R. Galan-Mascaros, C.J. Gomez-Garcia, J.M. Martinez-Agudo, *Inorg. Chem.* 40 (2001) 113.
- [9] F. Pointillart, C. Train, M. Gruselle, F. Villain, H.W. Schmalle, D. Talbot, P. Gredin, S. Decurtins, M. Verdager, *Chem. Mater.* 16 (2004) 832.
- [10] S. Decurtins, H.W. Schmalle, P. Schneuwly, J. Ensling, P. Gutlich, *J. Am. Chem. Soc.* 116 (1994) 9521.
- [11] S. Decurtins, H.W. Schmalle, R. Pellaux, P. Schneuwly, A. Hauser, *Inorg. Chem.* 35 (1996) 1451.
- [12] R. Sieber, S. Decurtins, H. Stoeckli-Evans, C. Wilson, D. Yufit, J.A.K. Howard, S.C. Capelli, A. Hauser, *Chem. Eur. J.* 6 (2000) 361.
- [13] H. Akutsu, A. Akutsu-Sato, S.S. Turner, P. Day, E. Canadell, S. Firth, R.J.H. Clark, J. Yamada, S. Nakatsuji, *Chem. Commun.* (2004) 18.
- [14] L. Martin, S.S. Turner, P. Day, P. Guionneau, J.A.K. Howard, D.E. Hibbs, M.E. Light, M.B. Hursthouse, M. Uruichi, K. Yakushi, *Inorg. Chem.* 40 (2001) 1363.
- [15] S. Decurtins, H.W. Schmalle, H.R. Oswald, A. Linden, J. Ensling, P. Gutlich, A. Hauser, *Inorg. Chim. Acta* 216 (1994) 65.
- [16] R. Pellaux, H.W. Schmalle, R. Huber, P. Fischer, T. Hauss, B. Ouladdiaf, S. Decurtins, *Inorg. Chem.* 36 (1997) 2301.
- [17] C. Mathoniere, C.J. Nuttall, S.G. Carling, P. Day, *Inorg. Chem.* 35 (1996) 1201.
- [18] T. Hashiguchi, Y. Miyazaki, K. Asano, M. Nakano, M. Sorai, H. Tamaki, N. Matsumoto, H. Okawa, *J. Chem. Phys.* 119 (2003) 6856.
- [19] A. Bhattacharjee, P. Gutlich, *J. Magn. Magn. Mater.* 268 (2004) 380.
- [20] E.I. Zhilyaeva, O.A. Bogdanova, R.N. Lyubovskaya, N.S. Ovanesyan, S.I. Pirumova, O.S. Roshchupkina, *Synth. Met.* 85 (1997) 1663.
- [21] R. Clement, S. Decurtins, M. Gruselle, C. Train, in: W. Linert, M. Verdager (Eds.), *Polyfunctional two- and three-dimensional oxalate-bridged bimetallic-based magnets, Molecular Magnets – Recent Highlights*, Springer Verlag, New York, 2003, pp. 1–20.
- [22] S. Decurtins, R. Pellaux, G. Antorrena, F. Palacio, *Coord. Chem. Rev.* 190–192 (1999) 841.
- [23] M. Pilkington, S. Decurtins, in: J.S. Miller, M. Drillon (Eds.), *Magnetism: Molecules to Materials II*, Wiley-VCH, Weinheim, 2001, pp. 339–356.
- [24] D. Lee, M.P. Suh, H. Bang, *J. Mol. Catal. A–Chem.* 151 (2000) 71.
- [25] C.A. Kelly, E.L. Blinn, N. Camaioni, M. D’Angelantonio, Q.G. Mulazzani, *Inorg. Chem.* 38 (1999) 1579.
- [26] Z.-L. Lu, C.-Y. Duan, Y.-P. Tian, X.-Z. You, *Inorg. Chem.* 35 (1996) 2253.
- [27] J.C. Bailar Jr., E.M. Jones, *Inorg. Synth.* 1 (1939) 35.
- [28] E.K. Barefield, F. Wagner, A.W. Herlinger, A.R. Dahl, *Inorg. Synth.* 16 (1976) 220.
- [29] Z.-L. Lu, C.-Y. Duan, Y.-P. Tian, X.-Z. You, H.-K. Fun, B.-C. Yip, *Polyhedron* 15 (1996) 1769.
- [30] Z. Otwinowsky, W. Minor, *Processing of X-ray Diffraction Data Collected in Oscillation Mode*, C.W. Carter Jr., R.M. Sweet (Eds.), *Methods Enzymol.* 276 (1996) 307–326.
- [31] G.M. Sheldrick, *Acta Crystallogr.* A46 (1990) 467.
- [32] G.M. Sheldrick, *SHELXL97. Program for the Crystal Structure Refinement*, University of Goettingen, Goettingen, Germany, 1997.
- [33] J. Huheey, in: *Inorganic Chemistry*, fourth ed., Harper Collins College Publishers, New York, 1993, Chapter 8, p. 292.